PERGAMON

International Journal of Heat and Mass Transfer 44 (2001) 1107–1117

International Journal of HEAT and MASS TRANSFER

www.elsevier.com/locate/ijhmt

Experimental study of natural convection in a square enclosure using differential interferometer

N. Ramesh, S.P. Venkateshan *

Department of Mechanical Engineering, Heat Transfer and Thermal Power Laboratory, Indian Institute of Technology, Madras 600 036, India

Received 27 August 1998; received in revised form 15 May 2000

Abstract

The results of an experimental study of laminar natural convection heat transfer in a square enclosure using air as the medium and having differentially heated isothermal vertical walls and adiabatic horizontal walls are reported. The study has been carried out using a differential interferometer (DI). After many trials, the authors have been able to achieve nearly adiabatic boundary conditions for top and bottom walls of the enclosure, in the laboratory environment. The study provides valuable information for many researchers – experimentalists or for those using numerical methods in analyzing problems of this type. A correlation for average convective Nusselt number is also provided.

1. Introduction

Natural convection heat transfer finds application in diverse areas such as solar energy systems, energy storage and conservation, fire research, nuclear reactor systems, materials processing, crystal growth. Heat transfer across vertical air layers is of practical importance especially in the estimation of heat transfer through double window glass panes, electronic equipment cooling, solar collectors, etc.

Studies on enclosures and partitioned enclosures are not new. However, the challenges for an experimentalist in realizing boundary conditions even for a simple geometry such as a square enclosure provides scope for further research. The literature survey on this class of problems is fairly exhaustive. Therefore, in this study, only those papers concerning enclosures are reviewed. Partitioned enclosures are not considered in this review. One of the earliest studies of natural convection in a differentially heated rectangular enclosure, subject to adiabatic boundary conditions at the top and bottom is due to Batchelor [1]. Batchelor obtained estimates of the Nusselt number in the conduction and transition regimes of flow, and a criterion for the change from one regime to the other was presented. It was concluded that, at sufficiently high Rayleigh numbers, the flow would consist of a core of constant temperature and vorticity, surrounded by a continuous boundary layer. Poots [2] obtained a numerical solution to the above problem. Poots solved the problem by expanding the stream function and the temperature in a series; a technique based on the use of orthogonal polynomials in order to obtain numerical approximations to the solution of the governing equations.

MacGregor and Emery [3] conducted experiments on rectangular enclosures of various aspect ratios (10, 20, 40). The experimental fluids were glycerin, castor oil, water and ethyl alcohol. The results for numerical computations including the case of variable properties were presented under isothermal wall and constant heat flux wall boundary conditions. Correlations for Nusselt number in terms of Rayleigh number, Prandtl number, and the aspect ratio were presented for both laminar and turbulent regimes. Eckert and Carlson [4] experimentally investigated the natural convection heat transfer between vertical isothermal walls of a rectangular enclosure, containing air. The temperature field inside the enclosure was obtained in great detail by a Mach–

* Corresponding author.
E-mail address: spv35@hotmail.com (S.P. Venkateshan).

0017-9310/01/$ - see front matter
PII: S0017-9310(00)00170-8

Nomenclature

d	width of the enclosure, m
g	acceleration due to gravity, m/s^2
Gr	Grashof number ($g\beta\Delta T d^3/v^2$), non-dimensional
h, $\overline{h}$	local and average convective heat transfer coefficients, respectively, at the hot wall, W/m^2 K
H	height of the hot wall or cold wall, m
k	thermal conductivity, W/m K
k_f	thermal conductivity of fluid (air) evaluated at T_m, W/m K
Nu_c	local convective Nusselt number (hd/k_f), non-dimensional
$\overline{N}u_c$	average convective Nusselt number ($\overline{h}d/k_f$), non-dimensional
Pr	Prandtl number of fluid (air), non-dimensional
T	temperature, °C or K
T_m	mean temperature $(T_h + T_c)/2$, °C or K
ΔT	temperature difference $(T_h - T_c)$, °C or K
x	coordinate along the height of the enclosure in the vertical direction, m
y	coordinate along the width of the enclosure in the horizontal direction, m

Greek symbols

β	volumetric expansion coefficient, K^{-1}
v	kinematic viscosity of fluid (air), m^2/s
θ	dimensionless temperature, $(T - T_c)/(T_h - T_c)$
ξ	dimensionless distance along the width, from the hot wall, y/H

Subscripts

b	bottom
c	cold
f	fluid
h	hot
m	mean
t	top

Zehnder interferometer. The aspect ratios considered were 2.5, 10 and 20. In the boundary layer regime, the core of the layer was not found to be isothermal; instead, the temperature was uniform along horizontal planes only and increased in the vertical direction, showing a stratified core. A correlation for mean Nusselt number as a function of Grashof number and aspect ratio was presented. No velocity measurements were made.

Elder [5] conducted experiments to study the natural convection heat transfer using medicinal paraffin and silicone oil in rectangular enclosures of different aspect ratios (12–60). Velocity measurements made by direct observation of aluminum powder suspended in the fluid were obtained in addition to the temperature measurements. The experiments confirmed the non-uniformity of the core temperature in the vertical direction. No correlations were reported from this study. Emery and Chu [6] analyzed natural convection in rectangular enclosures using experiments, and an integral method of analysis for fluids such as water, castor oil, glycerin, alcohol and red oil for two aspect ratios (10, 20). A correlation to predict the Nusselt number in terms of Rayleigh number and aspect ratio was presented. Elder [7] carried out a numerical study and compared the results with his earlier experimental work. An iterative procedure was employed to solve the governing equations.

Gill [8] developed a theory for the boundary layer regime for natural convection in a vertical rectangular cavity with differentially heated vertical walls and insulated top and bottom walls. The Gill solution was based first on the assumption that a stratified fluid core exists far away from both vertical walls. Boundary layer solutions were then obtained for the flow near the two vertical walls. Gill's solution fails to account for conditions very close to the top and bottom horizontal walls. This study was also largely based on the experimental observations of Elder [5].

de Vahl Davis [9] carried out a numerical study of the problem of natural convection between differentially heated vertical walls of a rectangular enclosure. Calculations were made for Rayleigh numbers up to 2×10^5 for a square cavity and up to 1.25×10^6 for a cavity with aspect ratio 5. Both linear temperature profile (LTP) and adiabatic boundary conditions for the top and bottom walls were considered in the study. Calculations were carried out using an 11×11 mesh, with 3, 5 and 7 point central-difference approximations. The Prandtl numbers were in the range $0.1 \leqslant Pr \leqslant 1000$.

Newell and Schmidt [10] performed a numerical analysis of air-filled enclosures of aspect ratios 1, 2.5, 10, and 20. The range $4\times10^3 \leqslant Gr \leqslant 1.4\times10^5$ was chosen for aspect ratios 1, 2.5, and 10 whereas $8\times10^3 \leqslant Gr \leqslant 4\times10^4$ was chosen for aspect ratio of 20. The time-dependent governing differential equations were solved using the Crank–Nicholson scheme. Correlations for the mean Nusselt number in terms of Grashof number and the aspect ratio were presented.

Berkovsky and Polevikov [11] carried out a numerical study of natural convection heat transfer in enclosures, using a higher order (fourth-order accurate) difference scheme for Rayleigh numbers of the order of 10^{10}–10^{12}. Correlations for Nusselt number as a function of Prandtl number, Rayleigh number and aspect ratio were presented.

Burnay et al. [12] experimentally studied natural convection inside a square enclosure. The study presented results for a very high Grashof number range,

which includes the onset of laminar instability, and is of particular interest in the study of air circulation at environmental room temperatures. A correlation for convective Nusselt number in terms of Grashof number was presented. Bejan [13] presented an extended study of the approximate solution provided by Gill [8]. The overall Nusselt number describing the net heat transfer by natural convection between the vertical walls of the enclosure was presented.

ElSherbiny et al. [14] reported the results of their measurements using air-filled enclosures of aspect ratios between 5 and 110 and Rayleigh number in the range $10^2 \leqslant Ra \leqslant 2\times10^7$. The air layer was bounded by flat isothermal plates at different temperatures and around the edges by a perfectly conducting boundary so that an LTP is created between the two isothermal plates. Correlating equations for calculating heat transfer across the air layer for both vertical and inclined enclosures were presented. de Vahl Davis [15] presented numerical results for a square cavity using the stream function–vorticity formulation. Forward-differences were used for the time derivatives and second-order central-differences were used for the spatial derivatives. The resulting finite-difference approximations were solved by an alternating-direction-implicit algorithm. The solution was allowed to evolve in time, to the steady state. No correlations were reported from the study. Only the values of Nusselt numbers for specific Rayleigh numbers were mentioned. The mesh size adopted was not constant; for small values of the Rayleigh number, for example, for $Ra = 10^3$, a 11×11 mesh was adopted and for higher values of Ra, the mesh size varied from 41×41 to as much as 81×81.

A two-dimensional, finite-difference method of analysis has been carried out by Zhong et al. [16] in a square enclosure, assuming black walls and considering variable properties and laminar natural convection, both with and without thermal radiation. A new correlation, based on the results of the numerical study, was also presented. It was also concluded that, while radiation is relatively insensitive to tilt angles, its effect on natural convection is considerable.

Balaji and Venkateshan [17], using a finite-volume method, performed a numerical study of natural convection in a square enclosure. The interaction of surface radiation with natural convection was studied in great detail. A 21×21 non-uniform grid was used in their study. The authors claimed that a three-point formula using a Lagrangian polynomial of degree 2, combined with a very fine grid near the walls enabled the derivative boundary conditions on the wall, less prone to error. Under-relaxation was used in solving the equations numerically. The study was carried out for the Grashof number range $10^3 \leqslant Gr \leqslant 10^6$. Balaji and Venkateshan [18] have presented correlations for evaluating the Nusselt number for a square cavity. The correlations also considered the effect of emissivity of all four walls of the cavity, thereby emphasizing the role played by surface radiation along with natural convection.

Shewen et al. [19] presented results for enclosures of very large aspect ratios such as 40, 60, and 110. Recently, Leong et al. [20] presented results for a natural convection problem of an air-filled cubical cavity. The results are presented for a cavity with one pair of opposing hot and cold walls, and the remaining faces having a linear variation of temperature. However, no correlations are reported in the paper.

From a survey of the literature, certain points are worthy of mention. Experimental studies on natural convection heat transfer in enclosures have been carried out for moderate to high aspect ratio enclosures. Moreover, air was not the general choice as the test fluid, but liquids such as water, castor oil, silicone oil, glycerin, red oil, etc., were used. In using fluids other than air, there was a considerable advantage to the experimenter in so far as realizing the adiabatic boundary conditions at the top and bottom walls were concerned. Maintaining adiabatic wall boundary conditions is extremely difficult, particularly if the test fluid is air.

There have been experimental studies on air-filled rectangular enclosures of moderate and high or very high aspect ratios. The correlations derived from the experiments and numerical studies on high aspect ratio enclosures were used to estimate the heat transfer across square cavities by assigning the value of aspect ratio term equal to 1. A large number of numerical studies have been carried out in rectangular enclosures; however, very few numerical studies on square enclosures are available. It is also of interest to note that, studies on enclosures reported in literature, choose either the height or the width of the enclosure as the characteristic dimension in order to obtain Grashof number or Rayleigh number. There is also a conflict among researchers regarding the effect of aspect ratio on the heat transfer rate across the enclosure. Ostrach [21] cautions the use of results from "similar" problems, saying "... natural convection is extremely sensitive to changes in the container configuration and the imposed boundary conditions so that the use of results from similar problems is dangerous."

The present work therefore attempts to provide answers to some of these issues. In the present work, an experimental study of laminar natural convection in a square cavity using differential interferometer (DI) is carried out. Two different insulating materials namely, non-rubberized cork ($k = 0.035$ W/m K) and Perspex™ ($k = 0.2$ W/m K) have been used as top and bottom walls enclosing an air layer in a square enclosure. Sufficient amount of glass wool ($k = 0.038$ W/m K) insulation (lagging) has been provided behind the top and bottom walls of the enclosure. By painstaking experiments, the present authors have been able to realize nearly adiabatic boundary conditions for the top and bottom

bounding walls of the enclosure in the laboratory environment.

2. Experimental apparatus and procedure

Two test cells were used in the present study in order to cover the required range of Grashof number values. Fig. 1 shows the sectional view of the 40 mm square test cell. The test section is a square enclosure 40 mm × 40 mm size and 200 mm deep in the direction of travel of the light beam of the interferometer. The second test cell is also a square enclosure having dimensions 60 mm × 60 mm × 300 mm. The hot and cold vertical walls were made of aluminum. The hot wall incorporates an electrical heater made of flat strip Nichrome™ wire carefully wound on a ruby mica sheet. Type K thermocouples were assembled in the hot and cold walls, at different locations along the length direction, in order to measure the temperature. The thermocouples were made of 0.3 mm diameter wire and were embedded in holes drilled very close to the polished surface of the wall. Aluminum powder mixed with Araldite™ was used for cementing purposes. The surface of the hot wall facing the cold wall was highly polished to a mirror finish in order to achieve a low emissivity of 0.05. The heater unit was energized by a stabilized ac power supply. The heater input was varied by means of a variable transformer.

A channel was milled in the cold wall in order to circulate constant temperature water provided by a thermostat (Haake F Junior, flow rate – 10 l/min, ±0.05°C) to act as a constant temperature sink. The surface of the cold wall facing the hot wall was also highly polished in order to achieve a mirror finish so as to have a low emissivity of 0.05. All thermocouples used in the present study were calibrated over the range of interest using a precision thermometer as reference and a constant temperature bath.

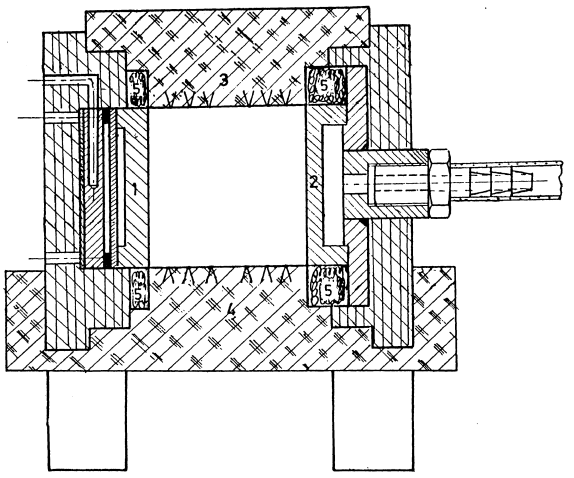

Fig. 1. Schematic diagram of the 40 mm × 40 mm experimental test cell (1 – hot wall, 2 – cold wall, 3 – top wall, 4 – bottom wall, 5 – glass wool insulation). The locations of thermocouples along the top and bottom walls are indicated thus >.

Two types of top and bottom walls were used in the present experiment. One set of walls were made of Perspex™ and the other made of non-rubberized cork. The top and bottom walls were also milled conforming to the required design. In arriving at the final design of the test cell, one of the most important considerations was to have a test cell such that there is no physical contact between the vertical walls and the horizontal walls. Slots were provided at all corners of the cell such that there is no conduction heat transfer across the hot/cold wall mounting boards and the top/bottom walls. After assembly, these slots were loosely filled with glass wool insulation material (see Fig. 1) in order to avoid air circulation in the slots. Care was taken during fabrication to ensure that the edges of the vertical walls do not touch the horizontal walls by providing a very small clearance (less than 1 mm) between the edges. Thermocouples were provided along the inside surfaces of the top and bottom walls also in order to measure the temperatures, as shown in the figure. In addition, thermocouples were also provided on the outside surface of the top wall to measure the top wall's outside surface temperature. This was done in order to estimate the heat loss via the top wall. (Discussion on this follows later, when Fig. 7 is taken up.)

The top and bottom walls were painted black (on the inside surfaces) in order to obtain a surface of emissivity of about 0.85 or provided with very thin aluminum foil (on the inside surfaces) so as to obtain a surface of emissivity of about 0.05, as the case may be, during the course of the experiments. For example, wooden walls [4] have an emissivity of about 0.85.

The front and rear sides of the enclosure were covered with optical quality glass plates with 3 mm nitrile rubber gasket between the edges of the walls and the glass plate. The rubber sheets, apart from providing a soft seating for the glass windows, avoid direct contact between the glass plate and the walls. The length of the test cell in the direction of the path of travel of light was 200 mm in the case of 40×40 mm^2 cell and 300 mm in the case of 60×60 mm^2 cell. This length, which is five times the height of the enclosure, ensures that two-dimensional conditions [22] prevail inside the enclosure. All sides of the enclosure (except the front and rear glass windows) were covered with glass wool insulation material up to a thickness of about 25 cm. This ensured that the conduction heat loss especially from the inside of the top wall to the outside was as small as possible. As mentioned earlier, this enabled the present authors to simulate nearly adiabatic top and bottom boundary conditions for the enclosure.

The optical instrument used to study the heat transfer phenomena is the DI (Spindler and Hoyer GmbH, Germany). Fig. 2 shows the schematic of the DI. The various parts of the interferometer are also given along with the figure. A detailed description of the DI is available elsewhere [23]. The core element of the DI is a shearing element providing a split of the incident wavefront into two wavefronts traveling through the test section separated by a definite distance. A Wollaston prism is used as the shearing element. The light from the mercury vapor lamp is allowed to pass through a condenser, heat filter, polarizer, interference filter (monochromator) and then through the partial mirror to a Wollaston prism in that order. The light exiting the biconvex lens (Fig. 2) is of high spectral quality satisfying the conditions necessary for interference. It is this light which is then allowed to pass through the test section. In the present study, light from green interference filter (549 nm) is chosen for analyzing the heat transfer phenomena. The biconvex lens provided a parallel beam of light to pass through the test section. These parallel rays were then made to retrace their path by means of the plane mirror. Both the biconvex lens as well as the plane mirror were fabricated out of optical quality glass. Aluminum was vapor deposited on the polished surface of the plane mirror glass blank to a thickness of a quarter wavelength. It was given an additional coating of silicon monoxide to make the surface scratch resistant.

The DI was calibrated before performing experiments on the square enclosure by the following procedure. One of the walls (cold wall of the enclosure) was considered to represent a vertical isothermal flat plate. The single vertical wall was carefully mounted in the path of the light beam and maintained at a predetermined temperature by means of the thermostat. The wall was thus allowed to lose heat by natural convection to the ambient air. A typical experiment was allowed to run for at least 4–5 h in order to ensure steady-state conditions. Photographs of the interferograms were recorded and the fringe deflections at various locations along the vertical wall were measured. The local convective heat transfer coefficients were then calculated from the measured fringe deflections using the procedure outlined elsewhere [23]. The local convective Nusselt numbers along the vertical wall were calculated and compared with the theoretical values obtained by similarity solution (due to Ostrach, as given in Chapman [24]). The comparison may be termed as excellent with the rms deviation of the experimental Nusselt number variation along the height being about 0.27 with respect to the theoretical Nusselt number variation. With respect to the mean Nusselt number, this translates to an error bar of ±4.2%. Fig. 3 shows graphically the result of the calibration experiment.

The walls of the enclosure were carefully positioned such that the interior angle was 90° at all corners. The test cell was perfectly aligned with a spirit level on a flat base with both the vertical walls in-line with the path of the light beam. The cold wall temperature was kept at a value slightly above the room temperature, ≅35°C. For a particular value of the cold wall temperature, the hot wall temperature was varied in steps from 50°C to 105°C. A typical experimental run lasted from about 10–12 h. Steady-state conditions were ensured before temperature readings were recorded. During the experiment, the temperature readings of points at identical locations both at the top wall and the bottom wall from two different cross-sectional locations along the depth of the enclosure were compared. It was found that a typical

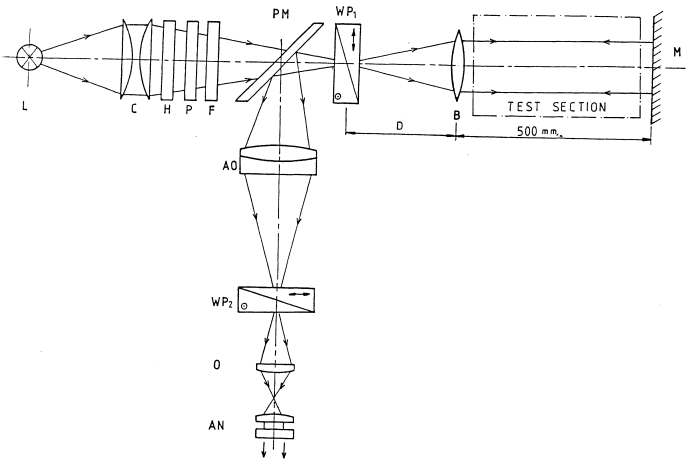

Fig. 2. Schematic of the DI. Diagram shows the optical components (L – light source, C – condenser, H – heat filter, P – polarizer, F – interference filter, PM – partial mirror, WP_1 – Wollaston prism, WP_2 – Wollaston prism, B – Biconvex lens, M – Plane mirror, AO – achromatic objective, O – ocular, AN – analyzer).

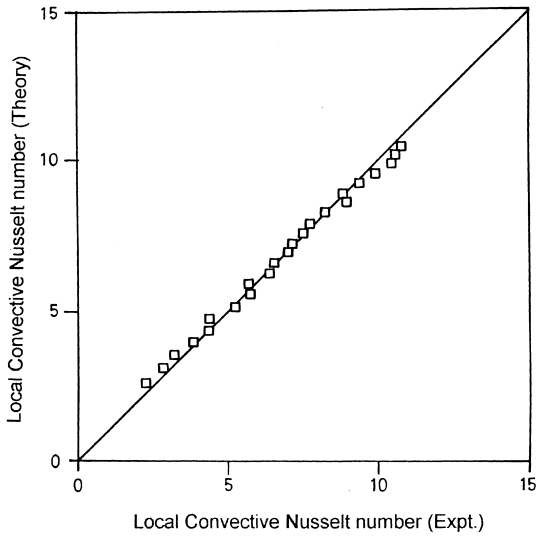

Fig. 3. Calibration curve for the DI. This curve is obtained for an isothermal vertical flat plate losing heat by natural convection, to air. The graph shows comparison of the experimental values of the local Nusselt number with the theoretical values obtained from similarity solution, due to Ostrach ($T_w = 59.5$°C, $T_\infty = 35.9$°C).

run for about 8 h was sufficient to obtain steady-state conditions. However, in the present study, each experimental run was allowed to continue for over 10 h as an extra insurance, to ensure steady-state conditions. Once the steady-state conditions were attained, temperatures of the walls and the photographs of the fringe field were recorded. The interferograms were recorded by means of an Asahi Pentax SLR camera with extension tube fitting for macro-photography on a Kodak Academy 200 ASA panchromatic film with suitable exposure settings.

3. Experimental uncertainty

There are only two types of measurement quantities associated with the present experiments that contribute to the overall uncertainty in the final result. These are the temperature and fringe deflection measurements. The uncertainty in temperature measurements is estimated to be within ±0.04°C and the uncertainty in fringe deflection measurement is estimated to be within ±0.02 mm. These would translate to an overall uncertainty in the estimated value of the convective Nusselt number to be less than ±3%.

4. Results and discussion

Fig. 4 shows the photograph of the typical interference fringe pattern with the wedge fringes. Similar

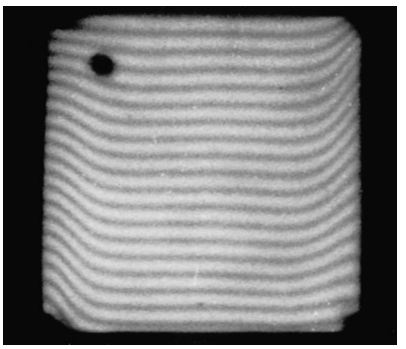

Fig. 4. Interference fringe pattern obtained from the interferometer. The photograph is for the square enclosure, for a typical experiment. The hot wall (left) was maintained at 103.3°C and the cold wall (right) at 34.7°C.

interferograms, obtained for various cases were made use of for the estimation of convective heat transfer coefficient. As mentioned earlier, the DI gives the value of the convective heat transfer coefficient along the surface by direct measurement of the fringe deflections at the surface of interest, from an interferogram, which is typically as shown in Fig. 4. The ratio of the fringe deflection to the fringe width at every location along the hot wall of the enclosure is then obtained in order to calculate the local heat transfer coefficient. The local heat transfer coefficients are integrated using trapezoidal rule in order to evaluate the average heat transfer coefficient. The fringe pattern across the horizontal walls can also be seen by suitable adjustment of the instrument. But due to core fluid stratification, the fringes are inclined from top to bottom of the core and because of this, the calculation of heat transfer coefficient for such cases will be in error. Hence, such an exercise was avoided.

Figs. 5(a) and (b) with infinite fringe setting (wedge fringes are absent in this setting) show the photograph of the free convective boundary layers adjacent to the hot/cold walls and top/bottom walls, respectively. A fringe line in this photograph corresponds to a line of constant gradient of the index of refraction and hence represents the constant gradient of the density, in a direction perpendicular to the walls. These lines therefore represent lines of constant conductive heat flux along both the walls. The same is true with Fig. 5(b). The symmetry of the boundary layers along the top and the bottom walls and also the existence of flow separation zones are clearly seen from the photograph shown in Fig. 5(b). The separated flow zones appear at two corners that are diametrically opposite to each other. These corners are the top corner of the hot vertical wall and the bottom corner of the cold vertical wall. These are regions where the rising hot fluid takes a turn to flow along the top wall from hot wall to cold wall and the

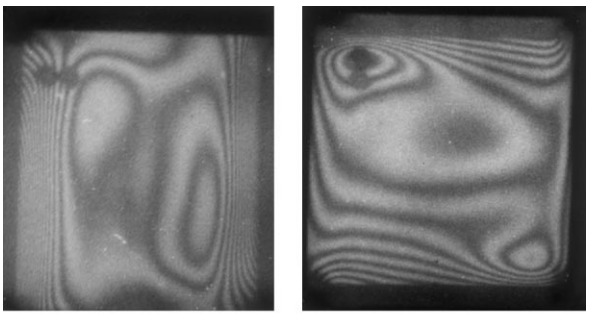

Fig. 5. (a) Constant heat flux lines shown by the interference pattern obtained for the infinite fringe setting of the DI. The boundary layers adjacent to the hot (left) and cold wall (right) can be seen. This photograph is for the same case shown in Fig. 4. (b) The boundary layers adjacent to the top and bottom bounding walls can be seen. Cork was chosen as the top and bottom bounding walls.

cold fluid takes a turn to flow along the bottom wall from cold wall to hot wall. It is to be noted that the photographs shown in Figs. 5(a) and (b) provide only a qualitative picture, and hence these photographs were never used for quantitative analysis, in order to estimate the convective heat transfer coefficient.

Fig. 6 shows the variation of the local convective heat transfer coefficient along the hot wall for a typical case. In the case of the hot wall in an enclosure, the boundary layer grows from bottom to top. This is similar to the case of a vertical isothermal flat plate loosing heat by natural convection to the ambient when the surface temperature is higher than the ambient. As expected, the local heat transfer coefficient has the highest value at the starting region of the boundary layer at the bottom of the wall, and decreases along the wall till it reaches the smallest value at or near the top of the wall. This can also be inferred from the photograph shown in Fig. 4, by a closer look at the points of deflection of the interference fringes near the hot wall. From the photograph, it can be seen that the deflection of the fringes is large near the bottom of the hot wall and small near the top region of the hot wall. A similar observation can be made for the case of the cold wall also, with 'top' and 'bottom' interchanged in the above statements. For perfect energy balance, the heat entering into the enclosure from the hot wall must equal the heat leaving the enclosure through the cold wall. This means, for any one experimental setting, the measurements of the fringe deflections along the hot and cold walls of the enclosure from a single interferogram should enable one to perform the energy balance. But, due to crowding of fringes near the top corner (see for example, Fig. 4) of the cold wall, it is difficult to estimate the total heat carried away by the cold wall. In order to circumvent this problem, the following procedure was adopted. At first, for one setting of the heater input, the enclosure was positioned so that the hot wall is on the left side. Then, for the same heater input, the enclosure was kept along the path of the light beam in such a way that the cold wall is on the left. For both cases, the interferograms were analyzed and energy balance was found to be satisfied within experimental errors.

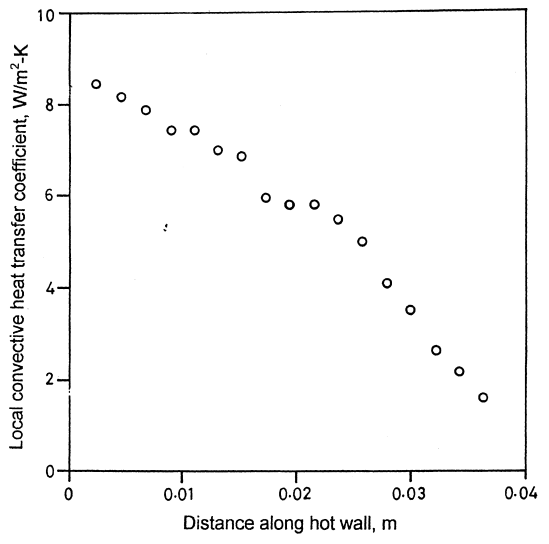

Fig. 6. Variation of the local heat transfer coefficient along the hot wall of the enclosure, for a typical experiment.

Fig. 7 shows the plot of the estimate of the heat loss from the top of the enclosure. The measured values of temperatures at various locations across the top wall of the enclosure on the outside surface were used in calculating the top heat loss by conduction using Fourier's law. It was found that the conduction heat loss increases as the temperature difference between the hot and cold walls of the enclosure increases. In this study, two types of insulation materials, viz., cork and Perspex™ were considered as candidate materials for the top and bottom walls. For the same amount of glass wool insulation provided on the outside of the enclosure, it was found

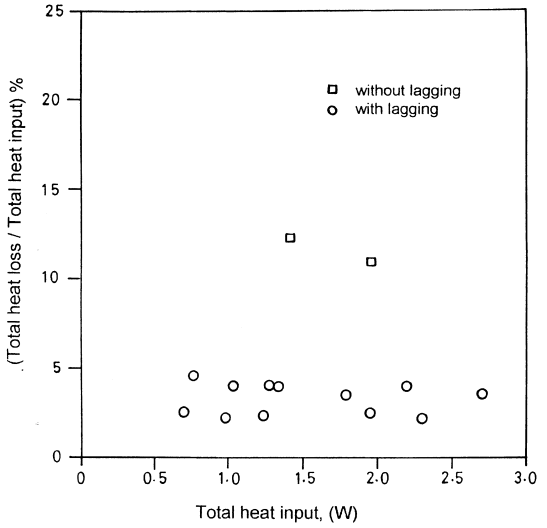

Fig. 7. Variation of the percentage heat loss from the top wall as a function of the total heat entering into the enclosure. The total heat entering into the enclosure is the sum total of the convective and radiative heat from the hot wall.

that there was very little increase in conduction heat loss if Perspex™ is used as the top wall material as compared to cork. The maximum temperature difference across the enclosure (i.e., ΔT) encountered in the present experimental study was 57.7°C. For this case, the average temperature on the inside surface of the top wall was 62.4°C while the average temperature on the outside of the top wall was 54.8°C; the difference being 7.7°C. For low values of the temperature difference between the hot and cold walls (ΔT), the average temperatures on the inside and outside surface of the top wall were in good agreement, which is an indication of very low conduction heat loss. The graph of Fig. 7 also has two data points, which show ≈11–12% heat loss. These data points are obtained for cases for which little or no glass wool insulation (lagging) was provided behind the walls of the enclosure. However, it can be concluded that by providing adequate lagging on the outside of the enclosure, the heat loss is minimized and nearly adiabatic boundary conditions are achievable. In the present experiments, the average heat loss for all the cases done with proper lagging on the outside of the enclosure was ≅3%.

The total heat entering into the enclosure from the hot wall is represented in the abscissa of the above figure. The average heat transfer coefficient multiplied by the surface area of the hot wall gives the total convective heat transfer into the enclosure from the hot wall. In order to calculate the radiative component of the heat transfer, it is necessary to know how each surface interacts with the other surfaces of the enclosure. In other words, the shape factors are to be evaluated. By dividing the inside walls of the enclosure into suitable number of small areas and by using Hottel's crossed string method [25], the shape factors were evaluated. Using the measured values of temperatures at various locations on all the walls and known emissivities of all surfaces, the radiative heat transfer from all the walls were calculated by using the method of enclosure analysis. The set of radiosity equations were solved using Gauss–Siedel iteration for calculating the radiative heat flux (see for example, [26]). The contribution of surface radiative heat transfer to the total heat transfer from the vertical isothermal hot wall was found to be negligibly small, and therefore not included in the calculation of the Nusselt number.

The variation of inside temperatures of the top and bottom walls along the width of the enclosure are shown in Fig. 8. The graphs are drawn using measured temperatures for the case in which cork was used for the top and bottom walls. The results of experiments done with and without glass wool insulation on the outside of the enclosure are shown. For both cases shown in the graph, the top wall temperatures are always higher than the bottom wall temperatures. Due to heat loss from the top, in an uninsulated case, the temperatures on the inside of the top wall of such an enclosure is very much lower than the corresponding case where adequate insulation is provided. The graph shows that even for a perfectly adiabatic case, the top and bottom temperatures vary linearly over a significant part excepting near the two corners. The two cases shown are for the same amount of electrical power input. Once again, the

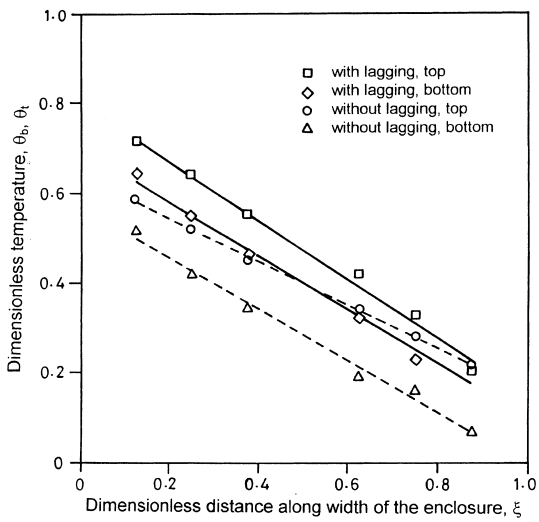

Fig. 8. Variation of the dimensionless top and bottom wall inside temperatures along the width of the enclosure from the hot wall side. Two cases are shown – one with lagging and the other without lagging on the outside of the enclosure.

importance of providing insulation on the outside can be clearly seen from the graph. It is interesting to note that the top temperature for the uninsulated enclosure approaches that of the insulated enclosure at locations very near the cold wall, where the temperature levels are comparatively lower than regions near the hot wall. It is worthy of mention that the inside flow and thermal transport phenomena are affected by the amount of insulation provided on the outside.

As mentioned earlier, in the present work, two different materials, viz., non-rubberized cork and Perspex™ of same thickness were used as candidate materials for the top and bottom bounding walls. Perspex™ is the usual choice of material for insulated walls in an enclosure in the laboratory experimental conditions due to the following two reasons: (i) the surface of perspex is smooth and perfectly flat, and (ii) ease of fabrication, especially when thermocouples are to be embedded. In fact, most experimental studies reported in the literature have made use of Perspex™. Our calculations showed that the difference in the Nusselt numbers obtained by using two different materials (cork vs Perspex™) were not significant to enable them to be categorically differentiated. However, Nusselt numbers obtained by using cork were slightly higher than those obtained with Perspex for all experiments. In the present study, experiments were performed for cases where top and bottom walls were coated with black board paint (so as to give an emissivity of 0.85) and also cases where the top and bottom walls were covered with very thin aluminum foil (so as to provide an emissivity of 0.05). The Nusselt numbers calculated for the two cases were found to be in good agreement and hence it was concluded that the emissivity of top and bottom walls do not affect significantly the values of Nusselt numbers. Fig. 9 shows the graph of the variation of the experimentally obtained values of mean convective Nusselt number with Grashof number.

The graph shown in Fig. 9 compares the present results with only those cases for which square cavity results are directly available. In plotting this graph, the correlation of Han [27] has been adopted as reported by Newell and Schmidt [10]. It can be seen from the graph that the results of the present study fall within the band covered by other numerical study results for a square cavity. Differences do exist among various numerical results, which cannot be ignored totally. Different numerical schemes use various order of accuracy methods in setting up difference equations in descretising the domain of interest. Moreover, the use of non-uniform or uniform grids, the use of relaxation parameter, simplifying assumptions, methods for ensuring stability at all Grashof numbers, convergence criteria contribute to the variation in results among numerical results themselves and with the present experimental results.

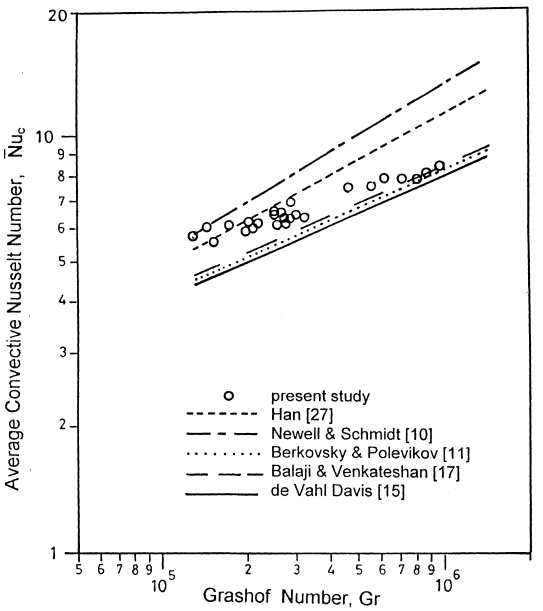

Fig. 9. Variation of mean convective Nusselt number with Grashof number. The mean Nusselt number obtained from the present study is compared with only those cases for which correlation for square cavity is available from literature.

5. Correlation

Based on experiments carried out, the following correlation for calculating the mean convective Nusselt number as a function of Grashof number is proposed. It is emphasized that only the convective Nusselt number is correlated. It was found that the radiative contribution from the hot wall was negligible due to the very low emissivity of the hot wall. Hence, the so-called radiative Nusselt number is not correlated. The mean Nusselt number is correlated as a function of Grashof number, given by $\overline{Nu} = 0.560Gr^{0.195}$ for the range $5\times10^4 \leqslant Gr \leqslant 2\times10^6$, wherein the fluid properties are evaluated at the mean of the hot and cold wall temperatures. The error band over the region of the correlation falls within the range, ±6%. The correlation coefficient is found to be 0.96. In most cases, the results of studies on enclosures using air, that are reported in literature, have used Grashof number as a parameter. In the present experimental study, we have used air as the fluid in the enclosure. The Prandtl number of air varies very little with temperature in the range of temperatures encountered in the present work. Hence, reporting results based on Grashof number is more appropriate. Fig. 10 shows the parity plot, which shows excellent agreement between experimental and correlated values of mean Nusselt number. It is hoped that this correlation will be useful to those working

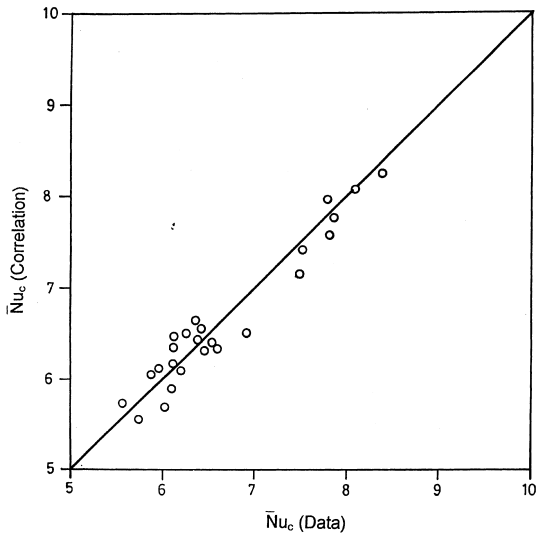

Fig. 10. Parity plot showing excellent agreement between experimental and correlated values of mean convective Nusselt number.

with numerical methods, especially for code validation purposes.

6. Conclusion

The results of the present study have brought to light certain subtle features inherent in the study of enclosure problems. The experimental study has been carried out by using an optical method with the help of a DI. Optical methods are reliable, considering the high fidelity that such instruments possess in replicating true phenomena. From the results obtained, it can be concluded without doubt that the flow and heat transfer characteristics inside the enclosure has a bearing on the boundary conditions on the outside. This is especially relevant in cases where air is used as the medium inside the enclosure.

The experience gained from the present investigation point to the fact that in order to achieve adiabatic boundary conditions as closely as possible, using air as the medium inside the enclosure, extra insulation (lagging) behind the walls should be provided, irrespective of the material used for the walls. Even though the study of natural convection in enclosures is not entirely new, often the need for an experimental correlation for a square enclosure with air as medium was felt by many, especially those who work with numerical methods. In practice, it has been observed that square enclosure is most sought for purposes of numerical code validation. The correlation developed in the present experimental study will be an excellent reference.

References

[1] G.K. Batchelor, Heat transfer by free convection across a closed cavity between vertical boundaries at different temperatures, Quart. Appl. Math. 12 (1954) 209–233.
[2] G. Poots, Heat transfer by laminar free convection in enclosed plane layers, Quart. J. Mech. Appl. Mech. 2 (1958) 257–273.
[3] R.K. MacGregor, A.F. Emery, Free convection through vertical plane layers – moderate and high Prandtl number fluids, ASME J. Heat Transfer 91 (1959) 391–403.
[4] E.R.G. Eckert, W.O. Carlson, Natural convection in an air layer enclosed between two vertical plates with different temperatures, Int. J. Heat Mass Transfer 2 (1961) 106–120.
[5] J.W. Elder, Laminar free convection in a vertical slot, J. Fluid Mech. 23 (1965) 77–98.
[6] A. Emery, N.C. Chu, Heat transfer across vertical layers, ASME J. Heat Transfer 87 (1965) 110–116.
[7] J.W. Elder, Numerical experiments with free convection in a vertical slot, J. Fluid Mech. 24 (1966) 823–843.
[8] A.E. Gill, The boundary-layer regime for convection in a rectangular cavity, J. Fluid Mech. 26 (1966) 515–536.
[9] G. De Vahl Davis, Laminar natural convection in an enclosed rectangular cavity, Int. J. Heat Mass Transfer 11 (1968) 1675–1693.
[10] M.E. Newell, F.W. Schmidt, Heat transfer by laminar natural convection within rectangular enclosures, ASME J. Heat Transfer 92 (1970) 159–168.
[11] B.M. Berkovsky, V.K. Polevikov, Numerical study of problems on high intensive free convection, in: D. Brian Spalding, N. Afgan (Eds.), Heat Transfer and Turbulent Buoyant Convection, Hemisphere, Washington, Vol. 2, 1977, pp. 443–455.
[12] G. Burnay, J. Hannay, J. Portier. Experimental study of free convection in a square cavity, in: D. Brian Spalding, N. Afgan (Eds.), Heat Transfer and Turbulent Buoyant Convection, Hemisphere, Washington, Vol. 2, 1977, pp. 807–811.
[13] A. Bejan, Note on Gill's solution for free convection in a vertical enclosure, J. Fluid Mech. 90 (1979) 561–568.
[14] S.M. ElSherbiny, G.D. Raithby, K.G.T. Hollands, Heat transfer by natural convection across vertical and inclined air layers, ASME J. Heat Transfer 104 (1982) 96–102.
[15] G.De. Vahl Davis, Natural convection of air in a square cavity. A bench mark numerical solution, Int. J. Num. Meth. Fluids. 3 (1983) 249–264.
[16] Z.Y. Zhong, K.T. Yang, J.R. Lloyd, Variable property natural convection in tilted enclosures with thermal radiation, in: R.W. Lewis, K. Morgan (Eds.), Numerical Methods in Heat Transfer, Vol 3, Wiley, New York, 1985, pp. 195–214.
[17] C. Balaji, S.P. Venkateshan, Interaction of surface radiation with free convection in a square cavity, Int. J. Heat Fluid Flow 14 (3) (1993) 260–267.
[18] C. Balaji, S.P. Venkateshan, Correlations for free convection and surface radiation in a square cavity, Int. J. Heat Fluid Flow. 15 (3) (1994) 249–251.
[19] E. Shewen, K.G.T. Hollands, G.D. Raithby, Heat transfer by natural convection across a vertical air cavity of large aspect ratio, ASME J. Heat Transfer. 118 (1996) 993–995.

[20] W.H. Leong, K.G.T. Hollands, A.P. Brunger, On a physically – realizable benchmark problem in internal natural convection, Int. J. Heat Mass Transfer 41 (1998) 3817–3828.
[21] S. Ostrach, Natural convection in enclosures, ASME J. Heat Transfer 110 (1988) 1175–1190.
[22] H. Ozoe, H. Sayama, S.W. Churchill, Natural convection in an inclined rectangular channel at various aspect ratios and angles – experimental measurements, Int. J. Heat Mass Transfer 18 (1975) 1425–1431.
[23] C.B. Sobhan, S.P. Venkateshan, K.N. Seetharamu, Experimental analysis of unsteady free convection heat transfer from horizontal fin arrays, Warme- und Stoffubertragung. 24 (1989) 155–160.
[24] A.J. Chapman, Heat Transfer, fourth ed., Macmillan, New York, 1989.
[25] H.C. Hottel, A.F. Sarofim, Radiative Heat Transfer, McGraw-Hill, New York, 1967.
[26] J.P. Holman, Heat Transfer, seventh ed., McGraw-Hill, New York, 1992.
[27] J.T. Han, Numerical solutions for an isolated vortex in a slot and free convection across a square cavity, MASc. Thesis, Department of Mechanical Engineering, University of Toronto, 1967.